Biogeosciences Discuss., 11, 10015–10043, 2014
www.biogeosciences-discuss.net/11/10015/2014/
doi:10.5194/bgd-11-10015-2014


Biogeosciences Discussions
Open Access



# Dependence of the cyclization of branched tetraethers (CBT) on soil moisture in the Chinese Loess Plateau and the adjacent areas: implications for palaeorainfall reconstructions

**H. Wang[1,2], W. Liu[1,3], and C. L. Zhang[4,5]**

[1]State Key Laboratory of Loess and Quaternary Geology, IEE, CAS, Xi'an, 710075, China
[2]University of Chinese Academy of Sciences, Beijing 100049, China
[3]School of Human Settlement and Civil Engineering, Xi'an Jiaotong University, Xi'an 710049, China
[4]State Key Laboratory of Marine Geology, Tongji University, Shanghai 200092, China
[5]Department of Marine Sciences, The University of Georgia, Athens, GA 30602, USA

Received: 11 January 2014 – Accepted: 16 June 2014 – Published: 27 June 2014

Correspondence to: W. Liu (liuwg@loess.llqg.ac.cn)

Published by Copernicus Publications on behalf of the European Geosciences Union.

## Abstract

Branched glycerol dialkyl glycerol tetraethers (bGDGTs) have been show promising for continental paleotemperature studies in loess-paleosol sequences (LPSs). Thus far, however, little is known about the effect of soil moisture on their distributions on the Chinese Loess Plateau (CLP). In this study, the relationships between environmental variables and the cyclization of bGDGTs (the so called CBT index) were investigated in a comprehensive set of surface soils in the CLP and its adjacent arid/semi-arid areas. We find that CBT correlates best with soil water content (SWC) or mean annual precipitation (MAP) for the total sample set. Particularly for the CLP soils, there is a significant positive relationship between CBT and MAP ($CBT = -0.0021 \cdot MAP + 1.7$, $n = 37$, $R^2 = 0.87$; MAP range: 210–680 mm). This indicates that CBT is mainly controlled by soil moisture in the alkalescent soils ($pH > 7$) in arid/semi-arid regions, where it is not sensitive to soil pH. Therefore, we suggest that CBT can potentially be used as a palaeorainfall proxy on the CLP.

According to the preliminary CBT–MAP relationship for modern CLP soils, palaeorainfall history was reconstructed from three LPSs (Yuanbao, Lantian, and Mangshan) with published bGDGT data spanning the past 70 ka. The CBT-derived MAP records of the three sites consistently show precession-driven variations resembling the speleothem $\delta^{18}O$ monsoon record, and are also in general accord with the fluctuations of the respective magnetic susceptibility (MS) record, supporting CBT as a reasonable proxy for palaeorainfall reconstruction in LPS studies. Moreover, the comparison of CBT-derived MAP and bGDGT-derived temperature may enable us to further assess the relative timing and magnitude of hydrological and thermal changes on the CLP, independent of chronology.

## 1 Introduction

The deposits of wind-blown dust (i.e. loess) on the Chinese Loess Plateau (CLP, Fig. 1) are some of the key nature archives of past climate changes. Characteristically, the plateau consists of a sequence of alternating loess and paleosol layers, which have accumulated at least since 2.6 Ma BP (Liu, 1985; Liu and Ding, 1998), with the records at places extending back to late Oligocene (Heller and Liu, 1982; Guo et al., 2002; Qiang et al., 2011). The cyclic alternation of loess and paleosol provides highly visible records of regional climate resulted from changing monsoon intensity on glacial-interglacial time scales (An, 2000 and references therein; Porter, 2001). For the past three decades, numerous proxies have been shown indicative of monsoon intensities in loess-paleosol sequences (LPSs), including: the traditional pedogenic magnetic susceptibility (Liu, 1985; Zhou et al., 1990; Maher et al., 1994) and grain size distributions (Ding et al., 1994, Sun et al., 2006), the geochemistry of iron oxides (Ding et al., 2001), the $\delta^{18}$O of rhizoconcretions and land snail shells (Li et al., 2007), the $\delta^{13}$C of total organic matter (An et al., 2005; Liu et al., 2005a, b; Ning et al., 2008; Rao et al., 2013) or carbonate (Liu et al., 2011), the $\delta^{13}$C and $\delta$D of leaf wax *n*-alkanes (Zhang et al., 2003, 2006; Liu and Huang, 2005; Liu et al., 2005b), phytolith (Lu et al., 2006, 2007), and trace mental ratios (Li and Li, 2014). The development of new palaeoclimatic proxies may further aid in the validation and explanations of the aforementioned proxies in the LPSs and the understanding of palaeoclimatic variations in monsoonal East Asia, and therefore, is still necessary for this climatologically important region.

Recent advantages in analytical methods using high performance liquid chromatography (HPLC)–mass spectrometry (MS) techniques enable the identification of a range of new lipid biomarkers-GDGTs (Hopmans et al., 2000; Sinninghe Damsté et al., 2000), as well as the subsequent understanding of their environmental occurrence and geochemical importance (reviewed in Schouten et al., 2013a). Particularly, the branched GDGTs (bGDGTs; Fig. 2) are ubiquitous in soils (Hopmans et al., 2004; Weijers et al., 2006a, 2007a; Sinninghe Damsté et al., 2008; Huguet et al., 2010; Tierney and Rus-





BGD
11, 10015–10043, 2014

sell, 2009; Peterse et al., 2009a, b, 2012; Loomis et al., 2011; Tierney et al., 2012; Yang et al., 2012, 2014a; Wang et al., 2013; Liu et al., 2013). They are presumed to origin from the cell membrane of unknown bacterial species (Weijers et al., 2006b; Sinninghe Damsté et al., 2011) with a heterotrophic lifestyle (Pancost and Sinninghe Damsté, 2003; Oppermann et al., 2010; Weijers et al., 2010). By the study of bGDGT distributions in > 130 globally soils, Weijers et al. (2007a) founded that the relative extent of cyclopentane moieties, expressed as the cyclisation ratio of bGDGTs (CBT), is negatively related to soil pH, whereas the degree of methylation for the nine bGDGTs, expressed as the methylation index of bGDGTs (MBT), is positively correlated with the mean annual air temperature (MAAT) and to some extent to soil pH. Therefore, paleo soil pH and MAAT can be quantified using CBT and the combination of MBT and CBT (MBT-CBT), respectively (Weijers et al., 2007a). An extended survey of 278 globally distributed surface soils further confirmed that CBT relates best to soil pH, while the simplified form of MBT (i.e. MBT' based on the seven most common bGDGTs) and CBT were shown correlating with MAAT (Peterse et al., 2012). Recently, Yang et al. (2014a) investigated the distribution of GDGTs in > 100 surface soils across a large climatic gradient of China, and proposed an alternative transfer function for MAAT reconstruction based on the fractional abundances of bGDGTs for use in semiarid and arid regions. This calibration has a markedly higher determination factor and lower root mean square error (RMSE) than the MBT/CBT proxy in alkaline soils (Yang et al., 2014a).

The sensitivity of soil bGDGT distributions to environmental variables offers new tools for quantitatively inferring past continental climate change in LPS studies. Initial application of the bGDGT paleothermometer to LPSs from the Mangshan (Peterse et al., 2011, 2014), Lantian (Gao et al., 2012), Yuanbao (Jia et al., 2013), and Weinan (Yang et al., 2014a, b) sections on the CLP indicates that bGDGTs might have recorded past changes in air temperature driven by local solar insolation. Unexpectedly, however, the CBT-reconstructed pH is higher for paleosol than for loess (Jia et al., 2013; Peterse et al., 2014), in contradiction with the well-accepted view that paleosol formed under wetter climate conditions. In fact, Xie et al. (2012) and Yang et al. (2014a) have recently observed a negative correlation between CBT and soil pH when pH < 7, but a slightly positive correlation or a flattening off when pH > 7, implying that some other factor(s) might have played an important role on CBT variations in alkalescent soils.

In the present study, we analyzed the CBT index in ca. 100 surface soils in the CLP and the adjacent arid/semi-arid areas with different climatic conditions. The aim of this work was to understand the environmental controls on soil CBT in the modern arid/semi-arid central China, in order to see if CBT can be used as a quantitative proxy specific for a certain environmental parameter in paleoclimate reconstructions in LPS studies.

## 2 Materials and methods

### 2.1 Regional setting and sample collection

The CLP is the largest region of loess deposits in the world. It is characterized by temperate semi-arid and semi-humid climate, modified by latitude, longitude, and terrain. Both the mean annual air temperature (MAAT) and the mean annual precipitation (MAP) show a clear northwestward decrease (Fig. 1). Dominated by the strength of the East Asian summer monsoon (EASM) system, the precipitation occurs mostly in the summer months (from May to September), which accounts for approximately 68–87 % of the total annual precipitation (Ding, 1994; Liu et al., 2005a). The present-day CLP is mainly covered by shrub (e.g., *Sophuora viciifolia and Vitex chinensis*) and grasses (e.g., *Artemisia and Gramineae*) (Liu, 1985). In general, the vegetation progressively becomes sparser and less dense from southeast to northwest, resulting from increasing dryness (Liu et al., 2005c).

A total of 97 samples were collected from 33 sites (i.e., 2–5 samples which are tens to hundreds of meters away for each site, except for site DengkouB with only one sample) in the CLP and the surrounding areas (Fig. 1). Samples for the CLP were collected from well-drained natural grassland (or to say the least, grassland restoration for > 10 years), and therefore are typical for local soils. For each sample, three randomly collected subsamples were pooled and mixed to make one composite sample representing that location. Most samples were collected from the uppermost layer of soil profiles with a depth of less than 5 cm and they were transported to the laboratory immediately after collection and stored at −20 °C. The detailed information of the samples is indicated in Supplement Table 1.

## 2.2 Environmental parameters

The SWC value for the sampling time was obtained by measuring sample weight before and after freeze drying.

Sample pH was measured following Wang et al. (2012): ca. 4 g freeze dried sample was added in 10 mL distilled water; the mixture was stirred for 1 min, left to stand for 30 min, and pH value of the supernatant was measured with a Sartorius PB-10 pH meter. The standard deviation for triplicate measurements was ± 0.03.

The meteorological data for our sampling sites were obtained from the China Meteorological Data Sharing Service System (http://cdc.cma.gov.cn/). MAP, MAAT, mean annual ground surface temperature (MAGST), mean annual relative humidity (RH), and mean annual evaporation (MAE) for each sampling site were estimated from the nearest climate stations. If there are 2–3 nearest stations for one sampling site, the meteorological data of them was averaged to generate an integrated meteorological data. Moreover, a further correction to the meteorological MAGST and MAAT values for each sample was made according to a lapse rate of −0.6 °C 100 $m^{-1}$.

## 2.3 Analysis of bGDGTs

The freeze dried and homogenized samples (30–50 g) were extracted (4 × 10 min) with dichloromethane (DCM) : methanol (9 : 1, v/v) using an accelerated solvent extractor (ASE 350, Dionex) at 100 °C and 1500 psi. The total extract was dried under $N_2$ in a water bath. A known amount of $C_{46}$ GDGT internal standard (IS, Huguet et al., 2006) was





BGD
11, 10015–10043, 2014

then added to the extract, which was redissolved in DCM : methanol (9 : 1, v/v) and divided into two halves. One half was dried under $N_2$, re-dissolved in hexane/isopropanol (99 : 1 v/v) and filtered over a 0.45 µm PTFE filter.

An aliquot (10 µL) of sample (100 or 600 µL, depending on GDGT concentration) was injected for HPLC-atmospheric pressure chemical ionization (APCI)-MS analysis according to a procedure slightly modified from Schouten et al. (2007) and Zhang et al. (2012). Separation of bGDGTs was achieved on an Alltech Prevail Cyano Column (150 mm × 2.1 mm, 3 µm). The elution gradient was: isocratic (5 min) at 99 % hexane/1 % isopropanol followed by a linear gradient to 1.8 % propanol in 45 min. After each analysis, the column was cleaned by back-flushing using 90 % hexane/10 % propanol. The flow rate was set at 0.2 mL $min^{-1}$. In order to increase sensitivity and reproducibility, selective ion monitoring (SIM) mode of the $[M + H]^+$ (protonated molecular ion) of the different bGDGTs (Fig. 2) was used to detect and quantify them. Quantification of each bGDGT was achieved by calculating the peak area in the chromatogram and comparing it with that of the IS. Ionization efficiency for bGDGTs and the IS was assumed identical.

The CBT index was calculated following Weijers et al. (2007a):

$$\text{CBT} = -\log \frac{\text{Ib} + \text{IIb}}{\text{I} + \text{II}}$$

Replicate analyses of 5 samples for CBT showed an averaging standard deviation of 0.01.

## 3 Results and discussion

### 3.1 Insensitivity of CBT to soil pH variation in alkalescent soils

Correlation of soil pH with CBT for surface soils in the CLP and the adjacent arid/semi-arid areas shows that there is a slight positive relationship between them at the pH range of 7.5–9 (Fig. 3; $R^2 = 0.25$, $N = 97$; $p < 0.01$). This seems different from the significant negative CBT–pH relationship observed regionally (Peterse et al., 2009b) and globally (Weijers et al., 2007a; Peterse et al., 2012). However, we note that the proportion of alkalescent soils (especially for soils with pH > 8) is much small in each calibration of the aforementioned studies. This consequently can modify the deviation of CBT values at higher pH values, if any, in the context of a large amount of soils with pH < 7. In fact, by extending the pH to > 9, Xie et al. (2012) and Yang et al. (2014a) have recently pointed out that the CBT index appears unable to distinguish pH variations in neutral to alkalescent soils, due to the weak positive CBT–pH relationship or a flattening-off of CBT when the pH is > 7, despite that the CBT values still exhibit a significant negative correlation with soil pH when pH < 7 (Fig. 3). The flattening-off of CBT at higher pH values was also observed by Peterse et al. (2010), who analyzed bGDGTs in long term soil pH manipulation plots in Scotland. Moreover, in lacustrine systems, a seemingly similar pattern was also obvious in the surface sediments of 23 lakes in China and Nepal (Sun et al., 2011), as well as in suspended particulate matter (SPM) from 23 lakes in the USA (Schoon et al., 2013). The weak correlation between CBT and pH under alkalescent conditions suggests that, variations in CBT might also be insensitive to changing pH in the alkalescent CLP soils.

The absence of a clear CBT–pH relationship under alkalescent conditions possibly reflects that a certain threshold is reached for bGDGT-producers in adapting their membrane lipids to pH. For the negative CBT–pH relationship, Weijers et al. (2007a) have proposed two likely mechanisms. Firstly, it is important for the microbes to maintain the internal pH within the cell constant, and therefore the bGDGT-producing bacteria tend to reduce the production of cyclopentyl moieties (causing higher CBT) at lower pH for better membrane packing and lower membrane permeability, which helps to protect cells against low pH (Weijers et al., 2007a). When pH is > 7, however, there seems no need for soil bacteria to overcome the inhibition of acidity. Secondly, the proton permeability (i.e., the pH gradient) of the cell membrane plays a crucial role in driving energy reactions over the cell membrane (e.g. Booth, 1985). Introduction of cyclopentyl





BGD
11, 10015–10043, 2014

moieties would enable more water molecules to get trapped in the membrane and consequently increases the membrane proton permeability, whereas a steeper proton gradient (thus lower ambient pH) is counteracted by a more impermeable membrane resulting from fewer cyclopentyl moieties and thus higher CBT (Weijers et al., 2007a). Under alkalescent conditions, however, further adaptation of the cell membrane would not be needed to overcome $H^+$ leakage (Schoon et al., 2013), if the bGDGT-producers turn to use $Na^+$ for energy transduction as neutrophiles and alkaliphiles, which are able to perform energy transduction by establishing a $Na^+$ gradient in combination with an $H^+$ gradient (Speelmans et al., 1995; Schoon et al., 2013). Overall, these could possibly explain the apparent insensitivity of CBT to pH in alkalescent conditions theoretically, and for the alkalescent CLP soils therefore, variations in CBT values should be attributed as a response to some factor(s) else.

### 3.2 Sensitivity of CBT to soil moisture in alkalescent soils

Notably in our dataset, we observed strong correlations of CBT with SWC (Table 1 and Fig. 4a; $R^2 = 0.46$, $N = 96$, $p < 0.01$) and MAP (Table 1 and Fig. 4b; $R^2 = 0.52$, $N = 97$, $p < 0.01$), which have much higher correlation coeficients than that for the CBT–pH relationship ($R^2 = 0.25$). The negative relationship between CBT and local MAP in our alkalescent soils is in accord with the results of Xie et al. (2012), at the MAP range of 200–800 mm (Fig. 5a). These empirical results imply that, in alkalescent soils, moisture conditions might have played an important role on CBT instead of soil pH. Contrarily, however, soil pH could have controlled CBT in acid to neutral soils, and therefore the positive correlation of MAP with CBT in Xie et al. (2012) when MAP > 800 is most likely a result of covariance with pH (Fig. 5b), which does not necessarily point to a direct causal relationship.

The most likely explanation for the negative CBT–SWC and CBT–MAP relationships in alkalescent soils might be that the formation of cyclopentane moieties could result in a loosening of the packing of the membrane lipids (Weijers et al., 2007a), whereas a dense packing of membrane lipids is needed to avoid over-evaporation of intracel-





BGD
11, 10015–10043, 2014

lular water from the membrane under dry conditions. However, as the exact biological source of bGDGTs is unknown, the reason why CBT correlates with soil moisture in alkalescent soils still remains speculative. Further studies of manipulation experiment would provide deeper insight into the exact physiological mechanism responsible for the observed moisture dependence of the CBT index.

We should note that our measured SWC is an instantaneous value that is liable to be affected by differences in the time of short-term local rainfall, and may not accurately stand for an average soil moisture condition during the growth of bGDGT producers. This might be an important factor causing the large scatter in the CBT–SWC relationship. For instance, typical soils in site Yongdeng (MAP: 284 mm) should be drier than those in the adjacent site Gulang (MAP: 352 mm). However, the measured SWC values for soils in Yongdeng (13, 13, and 12 %) collected immediately after a rainfall (according to our field note) were much higher than those for Gulang (3, 6, and 3 %). In such a case, the use of SWC at this sampling time could lead to an overestimation of the averaging soil moistures for bGDGT producers for Yongdeng (Fig. 4a). Omitting the Yongdeng samples, the CBT–MAP relationship was improved as expected ($R^2 = 0.56$). For extensive surface soil investigations therefore, variations in the SWC values at the time of sampling can only roughly reflect differences in mean soil moisture conditions.

MAP would be more representative for the mean soil moisture condition than the instantaneous SWC value, especially when local continuous observation data was not available for each sampling site. For the total dataset, however, CBT only correlates slightly better with MAP than with SWC. This is possibly because that the diversity in soil texture (e.g., desert sandy soils vs. CLP soils) can lead to different responses of soil moisture conditions to local MAP, causing the large scatter in the CBT–MAP relationship. Indeed, when further relevance analysis of CBT and MAP was performed only for the CLP soils, the positive CBT–MAP correlation exhibits a significant improvement ($R^2 = 0.87$, $N = 37$, $p < 0.01$). This might imply that soil texture should be taken into consideration when using meteorological MAP data for modern surface soil investigations.

The influence of temperature might not be a primary reason for the variations in CBT values. For the total dataset, we observed that CBT correlated substantially weakly ($R^2 = 0.02$, $N = 97$, $p = 0.13$) with mean annual ground surface temperature (MAGST). For the CLP samples, despite the significant correlation ($R^2 = 0.59$, $n = 37$, $p < 0.01$) observed for CBT with MAGST, the correlation is likely indirect since MAGST is also correlated with MAP ($R^2 = 0.62$, $n = 37$, $p < 0.01$) while the correlation coefficient of the CBT–MAP relationship is much higher than that of the CBT–MAGST relationship. Hence, the main factor controlling the CBT is suggested to be soil moisture (or MAP) for surface soils in the CLP and the adjacent arid/semi-arid areas.

### 3.3 Implications for palaeorainfall reconstruction on the CLP

The significant correlation between CBT and MAP in 37 surface soils on the CLP (Fig. 6a) indicates that this index may be a useful tool for palaeorainfall reconstruction in this region. The residual errors of the estimated MAP are < 127 mm, with a RMSE of 50 mm, and without following a clear trend with MAP (Fig. 6b). Analytically, the standard deviation for CBT is 0.01, equivalent to 6 mm of MAP, indicating that palaeorainfall estimates can be obtained with high analytical reproducibility.

In order to test the CBT index as a palaeorainfall proxy on the CLP, we applied it to three LPSs with published bGDGT data covering the past 70 kyr. Located from west to east on the southern CLP, the three LPSs are the Yuanbao (Fig. 7a, Jia et al., 2013), Lantian (Fig. 7b, Gao et al., 2012), and Mangshan (Fig. 7c, Peterse et al., 2014) sections, respectively. The CBT-derived MAP records exhibit pronounced precession-driven variations in rainfall amount at the three sites. Within dating uncertainties, the fluctuations of each record resembles the speleothem $\delta^{18}O$ record from the Hulu (Wang et al., 2001) and Sanbao (Wang et al., 2008) caves in southeast China (Fig. 7d), which are widely regarded as a robust record for the EASM intensity, predominantly for monsoon precipitation (Peterse et al., 2014). All these records indicate that rainfall amount was highest during Marine Isotope Stage (MIS) 1, relatively higher during MIS 3, and lowest during MIS 2 and probably MIS 4. In addition, the magnetic susceptibility

(MS) in LPSs has also been linked with climate, mainly through rainfall, by numerous investigators (Balsam et al., 2011 and references therein). For each section, the reconstructed rainfall history inferred from CBT is in general accord with the fluctuations of measured MS (Fig. 7a–c). Overall, the consistency of the CBT-inferred MAP records with other records of independent monsoon rainfall proxies (i.e., the speleothem $\delta^{18}O$ and MS records) strongly supports the CBT index as a palaeorainfall proxy on the CLP.

According the preliminary modern CBT–MAP calibration, the minimum MAP values for the three sites (559 mm, 726 mm, and 616 mm for Yuanbao, Lantian, and Mangshan, respectively) since the last glacial occurred at the Last Glacial Maximum (LGM), while the maximum values (780 mm, 834 mm, and 858 mm for Yuanbao, Lantian, and Mangshan, respectively) were reached during the Holocene, showing an overall ca. 200 mm enhancement in MAP on average during the transitional Deglacial period in the southern CLP. Moreover, the maximum and minimum values of reconstructed MAP for the Yuanbao LPS are much lower than those of Lantian and Mangshan LPSs, in agreement with the modern isohyets pattern of a decreasing MAP from east to west CLP (Fig. 1). However, these quantitative results based on CBT data measured by different laboratories should be interpreted with caution, since recent round-robin studies with dozens of laboratories have shown that GDGT indicies may vary significantly due to differences in inter-laboratory instrumental characteristics (Schouten et al., 2013b).

In view of the great potential of bGDGTs in reconstructing continental air temperature (Weijers et al., 2007a; Peterse et al., 2012; Yang et al., 2014a), the application of the CBT index derived from the same suite of lipids as a palaeorainfall proxy is particularly promising on the CLP. Recently, Peterse et al. (2014) proposed that the direct comparison of CBT-derived pH (likely precipitation-induced) and bGDGT-derived temperature might enable us to further assess the relative timing and magnitude of hydrological and thermal changes in continental east Asia, independent of potential biases associated with age model uncertainties. However, the reconstructed pH is unexpectedly higher in paleosol and weak paleosol (Peterse et al., 2014), which is in contrast to the presumption of Weijers et al. (2007b) that higher paleo-soil pH is related to drier conditions. In this study, the CBT–MAP relationship in alkalescent soils provides an empirical basis for the direct reconstruction of palaeorainfall based on the CBT index on the CLP, filling the gap of the uninterpretable results of previous studies (Jia et al., 2013; Peterse et al., 2014). The application of CBT as a palaeorainfall proxy in the three LPSs (Fig. 7a–c) confirms that continental air temperature and monsoon precipitation in southern CLP were generally decoupled (Peterse et al., 2011; 2014). The decoupling is more obvious for the past 30 kyr as the bGDGT results of each study exhibits an unambiguously lagged intensification of monsoon precipitation relative to Deglacial warming (Fig. 7a–c). This supports the idea that factors controlling the onset of Deglacial atmospheric warming and the intensification of East Asian Summer Monsoon might have been different (Peterse et al., 2011).

## 4 Summary

In this study, we have investigated the environmental controls on the CBT index for surface soils on the CLP and in the adjacent arid/semi-arid areas. In contrast to most previous studies covering a large range of soil pH values, no significant relationship was observed between soil pH and CBT for our data set. Further examination of other environmental factors showed that CBT is best correlated with SWC and MAP, indicating that soil moisture might have played an important role on the cyclisation ratio of bGDGTs in the alkalescent soils.

A preliminary calibration of MAP and CBT was established by 37 well-drained local natural soils on the CLP ($\mathrm{CBT} = -0.0021 \cdot \mathrm{MAP} + 1.7$). With a RMSE of 50 mm for the estimated MAP, this correlation might be useful for inferring past rainfall variations in this climatologically important region. According to this regional calibration, variations in reconstructed MAP based on three sets of published bGDGT data on the CLP (Yuanbao: Jia et al., 2013; Lantian: Gao et al., 2012; Mangshan: Peterse et al., 2014) are in agreement with the speleothem $\delta^{18}$O record and the fluctuations of site-specific MS, within age model uncertainties. The combination of the CBT rainfall indicator with the





BGD
11, 10015–10043, 2014

bGDGT temperature proxy derived from the same suite of lipids tells a similar story of the lag of monsoon precipitation relative to continental temperature (Peterse et al., 2011, 2014; Jia et al., 2013), independent of chronology. Moreover, the maximum and minimum values of reconstructed MAP for the drier Yuanbao section on the eastern CLP are systematically lower than those of the more humid Lantian and Mangshan sections on the western CLP. These evidences collectively support the CBT index as a palaeorainfall proxy on the CLP.

In conclusion, the results of this study indicate that CBT is a promising new palaeorainfall proxy on the CLP, although further research on the exact physiological mechanism and the additional data for a more accurate surface soil CBT–MAP calibration are required.

**The Supplement related to this article is available online at doi:10.5194/bgd-11-10015-2014-supplement.**

*Acknowledgements.* The China Meteorological Data Sharing Service System is thanked for providing free climatic data. This research was financially supported by the key deployment project from the Chinese Academy of Sciences (No. KZZD-EW-04-06), the national key funds of China (No. 2013CB955901), funds from the Chinese Academy of Sciences (No. XDA05120402), National Natural Science Foundation of China grants (No. 41030211), and the open fund of SKLLQG CAS (No. Y352000317). LC-MS analysis was performed in the State Key Laboratory of Marine Geology through the "National Thousand Talents Program" at Tongji University (CLZ).

## References


An, Z.: The history and variability of the East Asian paleomonsoon climate, Quaternary Sci. Rev., 19, 171–187, 2000.

An, Z., Huang, Y., Liu, W., Guo, Z., Clemens, S., Li, L., Prell, W., Ning, Y., Cai, Y., Zhou, W., Lin, B., Zhang, Q., Cao, Y., Qiang, X., Chang, H., and Wu, Z.: Multiple expansions of $C_4$ plant biomass in East Asia since 7 Ma coupled with strengthened monsoon circulation, Geology, 33, 705–708, 2005.

Balsam, W. L., Ellwood, B. B., Ji, J., Williams, E. R., Long, X., and El Hassani, A.: Magnetic susceptibility as a proxy for rainfall: worldwide data from tropical and temperate climate, Quaternary Sci. Rev., 30, 2732–2744, 2011.

Booth, I. R.: Regulation of cytoplasmic pH in bacteria, Microbiol. Rev., 359–378, 1985.

Ding, Y.: Monsoons Over China, Kluwer Academics Publishers, Dordrecht, 1994.

Ding, Z., Yang, S., Sun, J., and Liu, T.: Iron geochemistry of loess and red clay deposits in the Chinese Loess Plateau and implications for long-term Asian monsoon evolution in the last 7.0 Ma, Earth Planet. Sc. Lett., 185, 99–109, 2001.

Gao, L., Nie, J., Clemens, S., Liu, W., Sun, J., Zech, R., and Huang, Y.: The importance of solar insolation on the temperature variations for the past 110 kyr on the Chinese Loess Plateau, Palaeogeogr. Palaeocl., Palaeogeogr. Palaeoclimatol. Palaeoecol., 317–318, 128–133, 2012.

Guo, Z., Ruddiman, W. F., Hao, Q., Wu, H, Qiao, Y., Zhu, R., Peng, S., Wei, J., Yuan, B., and Liu, T.: Onset of Asian desertification by 22 Myr ago inferred from loess deposits in China, Nature, 416, 159–163, 2002.

Heller, F. and Liu, T.: Magnetostratigraphical dating of loess deposits in China, Nature, 300, 431–433, 1982.

Hopmans, E. C., Schouten, S., Pancost, R. D., van der Meer, M. T. J., and Sinninghe Damsté, J. S.: Analysis of intact tetraether lipids in archaeal cell material and sediments by high performance liquid chromatography/atmospheric pressure chemical ionization mass spectrometry, Rapid Commun. Mass Sp., 14, 585–589, 2000.

Hopmans, E. C., Weijers, J. W. H., Schefuss, E., Herfort, L., Sinninghe Damsté, J. S., and Schouten, S.: A novel proxy for terrestrial organic matter in sediments based on branched and isoprenoid tetraether lipids, Earth Planet. Sc. Lett., 224, 107–116, 2004.






BGD
11, 10015–10043, 2014

Dependence of the CBT on soil moisture in the Chinese Loess Plateau and the adjacent areas

H. Wang et al.

Huguet, A., Fosse, C., Metzger, P., Fritsch, E., and Derenne, S.: Occurrence and distribution of extractable glycerol dialkyl glycerol tetraethers in podzols, Org. Geochem., 41, 291–301, 2010.

Huguet, C., Hopmans, E. C., Febo-Ayala, W., Thompson, D. H., Sinninghe Damsté, J. S., and Schouten, S.: An improved method to determine the absolute abundance of glycerol dibiphytanyl glycerol tetraether lipids, Org. Geochem., 37, 1036–1041, 2006.

Huybers, P.: Early Pleistocene glacial cycles and the integrated summer insolation forcing, Science, 313, 508–511, 2006.

Jia, G., Rao, Z., Zhang, J., Li, Z., and Chen, F.: Tetraether biomarker records from a loessepaleosol sequence in the western Chinese Loess Plateau, Front. Microbiol., 4, 199, doi:10.3389/fmicb.2013.00199, 2013.

Li, G., Sheng, X., Chen, J., Yang, J., and Chen, Y.: Oxygen-isotope record of paleorainwater in authigenic carbonates of Chinese loess-paleosol sequences and its paleoclimatic significance, Palaeogeogr. Palaeocl., Palaeogeogr. Palaeoclimatol. Palaeoecol., 245, 551–559, 2007.

Li, T. and Li, G.: Incorporation of trace metals into microcodium as novel proxies for paleo-precipitation, Earth Planet. Sc. Lett., 386, 34–40, 2014.

Liu, T.: Loess and the Environment, China Ocean Press, Beijing, 1985.

Liu, T. and Ding, Z.: Chinese loess and the paleomonsoon. Annu. Rev. Earth Pl. Sc., 26, 111–145, 1998.

Liu, W. and Huang, Y.: Compound specific D/H ratios and molecular distributions of higher plant leaf waxes as novel paleoenvironmental indicators in the Chinese Loess Plateau, Org. Geochem., 36, 851–860, 2005.

Liu, W., Feng, X., Ning, Y., Zhang, Q., Cao, Y., and An, Z.: $\delta^{13}C$ variation of $C_3$ and $C_4$ plants across an Asian monsoon rainfall gradient in arid northwestern China, Global Change Biol., 11, 1094–1100, 2005a.

Liu, W., Huang, Y., An, Z., Clemens, S. C., Li, L., Prell, W. L., and Ning, Y.: Summer monsoon intensity controls $C_4/C_3$ plant abundance during the last 35 ka in the Chinese Loess Plateau: carbon isotope evidence from bulk organic matter and individual leaf waxes, Palaeogeogr. Palaeocl., Palaeogeogr. Palaeoclimatol. Palaeoecol., 220, 243–254, 2005b.

Liu, W., Ning, Y., An, Z., Wu, Z., Lu, H., and Cao, Y.: Carbon isotopic composition of modern soil and paleosol as a response of vegetation change in Loess Plateau, Sci. China Earth Sci., 48, 1, 93–99, 2005c.





BGD

11, 10015–10043, 2014

Dependence of the CBT on soil moisture in the Chinese Loess Plateau and the adjacent areas

H. Wang et al.

Liu, W., Yang, H., Sun, Y., and Wang, X.: $\delta^{13}$C values of loess total carbonate: a sensitive proxy for Asian summer monsoon in arid northwestern margin of the Chinese Loess Plateau, Chem. Geol., 284, 317–322, 2011.

Liu, W., Wang, H., Zhang, C. L., Liu, Z., and He, Y.: Distribution of glycerol dialkyl glycerol tetraether lipids along an altitudinal transect on Mt. Xiangpi, NE Qinghai-Tibetan Plateau, China, Org. Geochem., 57, 76–83, 2013.

Loomis, S., Russell, J., and Sinninghe Damsté, J. S.: Distributions of branched GDGTs in soils from western Uganda and implications for a lacustrine paleothermometer, Org. Geochem., 42, 739–751, 2011.

Lu, H., Wu, N., Yang, X., Jiang, H., Liu, K., and Liu, T.: Phytoliths as quantitative indicators for the reconstruction of past environ mental conditions in China I: Phytolith-based transfer functions, Quaternary Sci. Rev., 25, 945–959, 2006.

Lu, H., Wu, N., Liu, K., Jiang, H., and Liu, T.: Phytoliths as quantitative indicators for the reconstruction of past environmental conditions in China II: Palaeoevironmental reconstruction in the Loess Plateau, Quaternary Sci. Rev., 26, 759–772, 2007.

Maher, B., Thompson, R., and Zhou, L.: Spatial and temporal reconstructions of changes in the Asian palaeomonsoon: a new mineral magnetic approach, Earth Planet. Sc. Lett., 125, 461–471, 1994.

Ning, Y., Liu, W., and An, Z.: A 130-ka reconstruction of precipitation on the Chinese Loess Plateau from organic carbon isotopes, Palaeogeogr. Palaeocl., 270, 59–63, 2008.

Oppermann, B. I., Michaelis, W., Blumenberg, M., Frerichs, J., Schulz, H.-M., Schippers, A., Beaubien, S. E., and Krüger, M.: Soil microbial community changes as a result of long-term exposure to a natural $CO_2$ vent, Geochim. Cosmochim. Ac., 74, 2697–2716, 2010.

Pancost, R. D. and Sinninghe Damsté, J. S.: Carbon isotopic compositions of prokaryotic lipids as tracers of carbon cycling in diverse settings, Chem. Geol., 195, 29–58, 2003.

Peterse, F., Kim, J.-H., Schouten, S., Klitgaard Kristensen, D., Koç, N., and Sinninghe Damsté, J. S.: Constraints on the application of the MBT/CBT paleothermometer in high latitude environments (Svalbard, Norway), Org. Geochem., 40, 692–699, 2009a.

Peterse, F., van der Meer, M. T. J., Schouten, S., Jia, G., Ossebaar, J., Blokker, J., and Sinninghe Damsté, J. S.: Assessment of soil *n*-alkane $\delta$D and branched tetraether membrane lipid distributions as tools for paleoelevation reconstruction, Biogeosciences, 6, 2799–2807, doi:10.5194/bg-6-2799-2009, 2009b.

Peterse, F., Nichol, G., Schouten, S., and Sinninghe Damsté, J. S.: Influence of soil pH on the abundance and distribution of core and intact polar lipid-derived branched GDGTs in soil, Org. Geochem., 41, 1171–1175, 2010.

Peterse, F., Prins, M. A., Beets, C. J., Troelstra, S. R., Zheng, H., Gu, Z., Schouten, S., and Sinninghe Damsté, J. S.: Decoupled warming and monsoon precipitation in East Asia over the last deglaciation, Earth Planet. Sc. Lett., 301, 256–264, 2011.

Peterse, F., van der Meer, J., Schouten, S., Weijers, J. W. H., Fierer, N., Jackson, R. B., Kim, J.-H., and Sinninghe Damsté, J. S.: Revised calibration of the MBT-CBT paleotemperature proxy based on branched tetraether membrane lipids in surface soils, Geochim. Cosmochim. Ac., 96, 215–229, 2012.

Peterse, F., Martínez-García, A., Zhou, B., Beets, C. J., Prins, M. A., Zheng, H., and Eglinton, T. I.: Molecular records of continental air temperature and monsoon precipitation variability in East Asia spanning the past 130,000 years, Quaternary Sci. Rev., 83, 1–7, 2014.

Porter, S. C.: Chinese loess record of monsoon climate during the last glacial-interglacial cycle, Earth-Sci. Rev., 54, 115–128, 2001.

Qiang, X., An, Z., Song, Y., Chang, H., Sun, Y., Liu, W., Ao, H., Dong, J., Fu, C., Wu, F., Lu, F., Cai, Y., Zhou, W., Cao, J., Xu, X., and Ai, L.: New eolian red clay sequence on the western Chinese Loess Plateau linked to onset of Asian desertification about 25 Ma ago, Sci. China Earth Sci., 54, 136–144, 2011.

Rao, Z., Chen, F., Cheng, H., Liu, W., Wang, G., Lai, Z., and Bloemendal, J.: High-resolution summer precipitation variations in the western Chinese Loess Plateau during the last glacial, Scientific Reports, 3, 2785, doi:10.1038/srep02785, 2013.

Schoon, L., de Kluijver, A., Middelburg, J. J., Downing, J. A., Sinninghe Damsté, J. S., Schouten, S.: Influence of lake water pH and alkalinity on the distribution of core and intact polar branched glycerol dialkyl glycerol tetraethers (GDGTs) in lakes, Org. Geochem., 60, 72–82, 2013.

Schouten, S., Huguet, C., Hopmans, E. C., and Sinninghe Damsté, J. S.: Improved analytical methodology of the $TEX_{86}$ palaeothermometry by high performance liquid chromatography/atmospheric pressure chemical ionization-mass spectrometry, Anal. Chem., 79, 2940–2944, 2007.

Schouten, S., Hopmans, E. C., and Sinninghe Damsté, J. S.: The organic geochemistry of glycerol dialkyl glycerol tetraether lipids: a review, Org. Geochem., 54, 19–61, 2013a.

Schouten, S., Hopmans, E. C., Rosell-Melé, A., Pearson, A., Adam, P., Bauersachs, T., Bard, E., Bernasconi, S., Bianchi, T. S., Brocks, J. J., Truxal-Carlson, L., Castañeda, I. S., Dutta, K., Eglinton, T., Fosse, C., Grice, K., Hinrichs, K. E., Huang, Y., Huguet, A., Huguet, C., Hurley, S., Ingalls, A., Jia, G., Keely, B., Knappy, C., Lincoln, S., Lipp, J., Mangelsdorf, K., Martinez-Garcia, A., van-der-Meer, J., Ménot-Combes, G., Mets, A., Mollenhauer, G., Ohkouchi, N., Ossebaar, J., Pagani, M., Pancost, R. D., Pearson, E. J., Peterse, F., Reichart, G. J., Schaeffer, P., Schmitt, G., Selver, A. D., Shah, S. R., Smith, R. W., Smittenberg, R., Takano, Y., Talbot, H. M., Taylor, K. W. R., Tarozo, R., Van-Dongen, B. E., Van-Mooy, B. A. S., Weijers, J. W. H., Werne, J. P., Woltering, M., Xie, S., Yamamoto, M., Yang, H., Zhang, C., Zhao, M., and Sinninghe Damsté, J. S.: An interlaboratory study of $TEX_{86}$ and BIT analysis of sediments, extracts and standard mixtures, Geochem. Geophy. Geosy., 11, 5263–5285, doi:10.1002/2013GC004904, 2013b.

Sinninghe Damsté, J. S., Hopmans, E. C., Pancost, R. D., Schouten, S., and Geenevasen, J. A. J.: Newly discovered non-isoprenoid dialkyl diglycerol tetraether lipids in sediments, J. Chem. Soc. Chem. Comm., Journal of the Chemical Society, Chem. Commun., 23, 1683–1684, 2000.

Sinninghe Damsté, J. S., Ossebaar, J., Schouten, S., and Verschuren, D.: Altitudinal shifts in the distribution of branched tetraether lipids in soils from Mt. Kilimanjaro (Tanzania): implications for the MBT/CBT continental palaeothermometer, Org. Geochem., 39, 1072–1076, 2008.

Sinninghe Damsté, J. S., Rijpstra, W. I. C., Hopmans, E. C., Weijers, J. W. H., Foesel, B. U., Overmann, J., and Dedysh, S. N.: 13,16-Dimethyl octacosanedioic acid (iso-diabolic acid): a common membrane-spanning lipid of Acidobacteria subdivisions 1 and 3, Appl. Environ. Microb., 77, 4147–4154, 2011.

Speelmans, G., Poolman, B., and Konings, W. N.: $Na^+$ as coupling ion in energy transduction in extremophilic bacteria and archaea, World J. Microb. Biot., 11, 58–70, 1995.

Sun, Q., Chu, G., Liu, M., Xie, M., Li, S., Ling, Y., Wang, X., Shi, L., Jia, G., and Lu, H.: Distributions and temperature dependence of branched glycerol dialkyl glycerol tetraethers in recent lacustrine sediments from China and Nepal, J. Geophys. Res., 116, G01008-1–G01008-12, 2011.

Sun, Y., Clemens, S. C., An, Z., and Yu, Z.: Astronomical timescale and palaeoclimatic implication of stacked 3.6-Ma monsoon records from the Chinese Loess Plateau, Quaternary Sci. Rev., 25, 33–48, 2006.





BGD
11, 10015–10043, 2014

Dependence of the CBT on soil moisture in the Chinese Loess Plateau and the adjacent areas

H. Wang et al.

Tierney, J. E. and Russell, J. M.: Distributions of branched GDGTs in a tropical lake system: implications for lacustrine application of the MBT/CBT palaeoproxy, Org. Geochem., 40, 1032–1036, 2009.
Tierney, J. E., Schouten, S., Pitcher, A., Hopmans, E. C., and Sinninghe Damsté, J. S.: Core and intact polar glycerol dialkyl glycerol tetraethers (GDGTs) in Sand Pond, Warwick, Rhode Island (USA): insights into the origin of lacustrine GDGTs, Geochim. Cosmochim. Ac., 77, 561–581, 2012.
Wang, H., Liu, W., Zhang, C. L., Wang, Z., Wang, J., Liu, Z., and Dong, H.: Distribution of glycerol dialkyl glycerol tetraethers in surface sediments of Lake Qinghai and surrounding soil, Org. Geochem., 47, 78–87, 2012.
Wang, H., Liu, W., Zhang, C., Liu, Z., and He, Y.: Branched and isoprenoid tetraether (BIT) index traces water content along two marsh-soil transects surrounding Lake Qinghai: implications for paleo-humidity variation, Org. Geochem., 59, 79–81, 2013.
Wang, Y., Cheng, H., Edwards, R. L., An, Z., Wu, J., Shen, C., and Dorale, J. A.: A high-resolution absolute-dated Late Pleistocene monsoon record from Hulu Cave, China, Science, 294, 2345–2348, 2001.
Wang, Y., Cheng, H., Edwards, R., Kong, X., Shao, X., Chen, S., Wu, J., Jiang, X., Wang, X., and An, Z.: Millennial- and orbital-scale changes in the East Asian monsoon over the past 224,000 years, Nature, 451, 1090–1093, 2008.
Weijers, J. W. H., Schouten, S., Spaargaren, O. C., and Sinninghe Damsté, J. S.: Occurrence and distribution of tetraether membrane in soils: implications for the use of the BIT index and the TEX86 SST proxy, Org. Geochem., 37, 1680–1693, 2006a.
Weijers, J. W. H., Schouten, S., Geenevasen, J. A. J., David, O. R. P., Coleman, J., Pancost, R. D., and Sinninghe Damsté, J. S.: Membrane lipids of mesophilic anaerobic bacteria thriving in peats have typical archaeal traits, Environ. Microb., 8, 648–657, 2006b.
Weijers, J. W. H., Schouten, S., van Den Donker, J. C., Hopmans, E. C., and Sinninghe Damsté, J. S.: Environmental controls on bacterial tetraether membrane lipid distribution in soils, Geochim. Cosmochim. Ac., 71, 703–713, 2007a.
Weijers, J. W. H., Schefuss, E., Schouten, S., and Sinninghe Damsté, J. S.: Coupled thermal and hydrological evolution of tropical Africa over the last deglaciation, Science, 315, 1701–1704, 2007b.
Weijers, J. W. H., Wiesenberg, G. L. B., Bol, R., Hopmans, E. C., and Pancost, R. D.: Carbon isotopic composition of branched tetraether membrane lipids in soils suggest a rapid turnover





BGD
11, 10015–10043, 2014

Dependence of the CBT on soil moisture in the Chinese Loess Plateau and the adjacent areas

H. Wang et al.

and a heterotrophic life style of their source organism(s), Biogeosciences, 7, 2959–2973, doi:10.5194/bg-7-2959-2010, 2010.
Xia, D., Jia, J., Wei, H., Liu, X., Ma, J., Wang, X., and Chen, F.: Magnetic properties of surface soils in the Chinese Loess Plateau and the adjacent Gobi areas, and their implication for climatic studies, J. Arid Environ., 78, 73–79, 2012.
Xie, S., Pancost, R. D., Chen, L., Evershed, R. P., Yang, H., Zhang, K., Huang, J., and Xu, Y.: Microbial lipid records of highly alkaline deposits and enhanced aridity associated with significant uplift of the Tibetan Plateau in the Late Miocene, Geology, 40, 291–294, 2012.
Yang, H., Ding, W., Wang, J., Jin, C., He, G., Qin, Y., and Xie, S.: Soil pH impact on microbial tetraether lipids and terrestrial input index (BIT) in China, Sci. China Earth Sci., 55, 236–245, 2012.
Yang, H., Pancost, R. D., Dang, X., Zhou, X., Evershed, R. P., Xiao, G., Tang, C., Gao, L., Guo, Z., and Xie, S.: Correlations between microbial tetraether lipids and environmental variables in Chinese soils: optimizing the paleo-reconstructions in semi-arid and arid regions, Geochim. Cosmochim. Ac., 126, 49–69, 2014a.
Yang, H., Pancost, R. D., Tang, C., Ding, W., Dang, X., and Xie, S.: Distributions of isoprenoid and branched glycerol dialkanol diethers in Chinese surface soils and a loess–paleosol sequence: implications for the degradation of tetraether lipids, Org. Geochem., 66, 70–79, 2014b.
Zhang, C. L. Wang, J., Wei, Y., Zhu, C., Huang, L., and Dong, H.: Production of branched tetraether lipids in the lower Pearl River and estuary: effects of extraction methods and impact on bGDGT proxies, Front. Microbiol., 2, 274, doi:10.3389/fmicb.2011.00274, 2012.
Zhang, Z., Zhao, M., Lu, H., and Faiia, A. M.: Lower temperature as the main cause of $C_4$ plant declines during the glacial periods on the Chinese Loess Plateau, Earth Planet. Sc. Lett., 214, 467–481, 2003.
Zhang, Z., Zhao, M., Eglinton, G., Lu, H., and Huang, C.: Leaf wax lipids as paleovegetational and paleoenvironmental proxies for the Chinese Loess Plateau over the last 170 kyr, Quaternary Sci. Rev., 25, 575–594, 2006.
Zhou, L., Oldfield, F., Wintle, A. G., Robinson, S. G., and Wang, J.: Partly pedogenic origin of magnetic variations in Chinese loess, Nature, 346, 737–739, 1990.

**Table 1.** Correlation coefficients (*R*) for CBT and environmental variables including altitude, soil pH, SWC, MAP, MAGST, RH, MAAT and MAE. $R > 0.6$ or $< -0.6$ are indicated in bold.

| | altitude | Soil pH | SWC | MAP | MAGST | RH | MAAT | MAE | CBT |
|---|---|---|---|---|---|---|---|---|---|
| altitude | 1.00 | | | | | | | | |
| Soil pH | −0.01 | 1.00 | | | | | | | |
| SWC | −0.21 | **−0.63** | 1.00 | | | | | | |
| MAP | −0.24 | **−0.66** | **0.89** | 1.00 | | | | | |
| MAGST | **−0.69** | 0.13 | 0.17 | 0.26 | 1.00 | | | | |
| RH | −0.19 | −0.47 | **0.69** | **0.81** | 0.36 | 1.00 | | | |
| MAAT | **−0.77** | 0.06 | 0.26 | 0.35 | **0.98** | 0.37 | 1.00 | | |
| MAE | −0.03 | 0.40 | −0.57 | **−0.70** | −0.24 | **−0.91** | −0.24 | 1.00 | |
| CBT | 0.37 | 0.50 | **−0.68** | **−0.72** | −0.16 | −0.46 | −0.28 | 0.27 | 1.00 |





BGD
11, 10015–10043, 2014

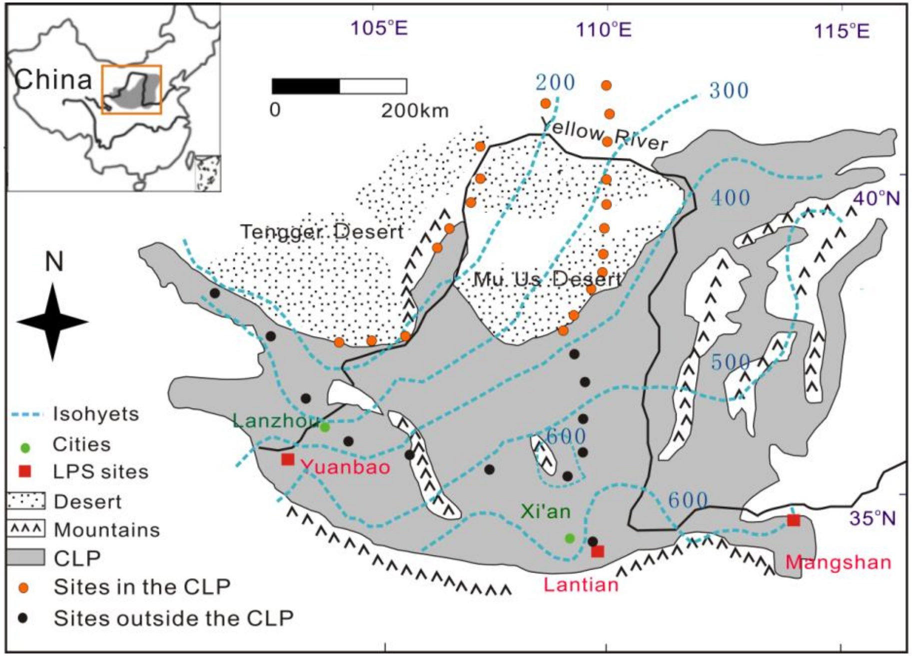


**Figure 1.** Sketch map of the CLP and its surroundings showing the locations of samples used for a regional investigation of CBT and the environmental controls (modified from Xia et al., 2012). The sites of three LPS sections with published bGDGT data (Yuanbao, Lantian and Mangshan) are also shown. The relative position of the study region in China is indicated in the upper-left.

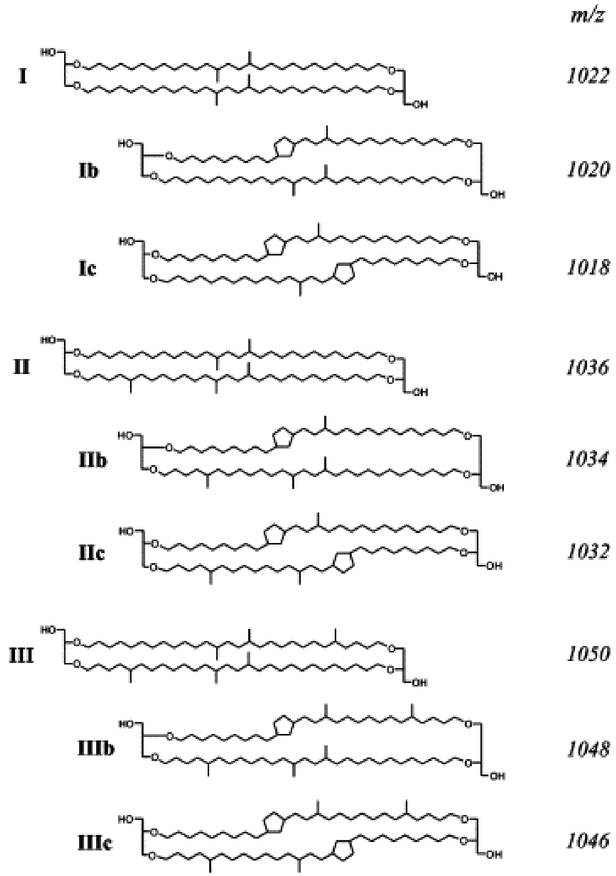


**Figure 2.** Molecular structures of bGDGTs and the mass to charge ratios of protonated molecular ions (after Weijers et al., 2007a).

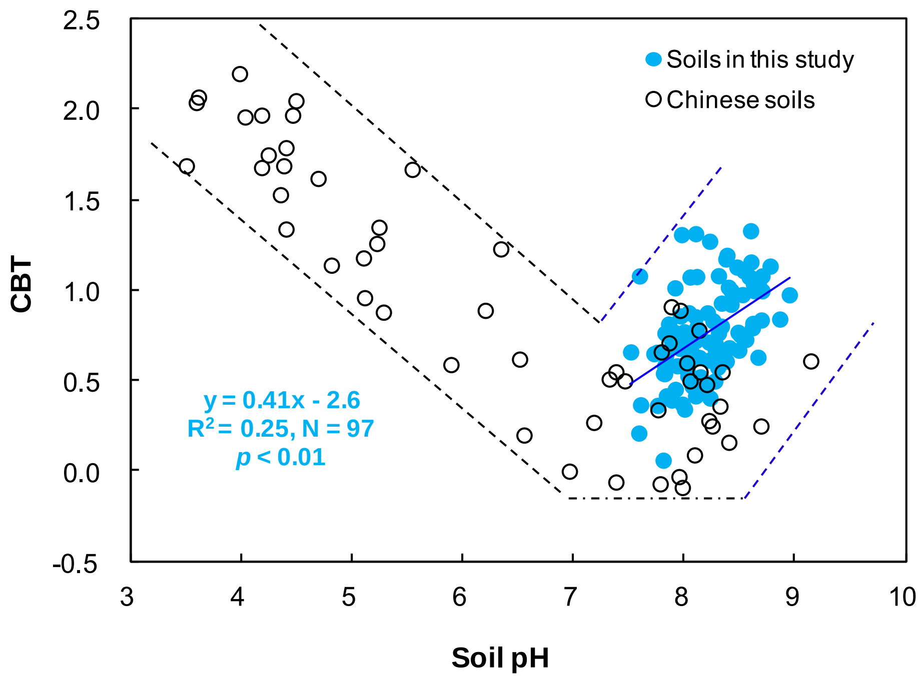


**Figure 3.** Plot of soil pH vs. CBT for surface soil samples on the CLP and the adjacent arid/semi-arid areas. Also shown is the correlation between pH and CBT in Chinese soils reported previously (Xie et al., 2012).





BGD
11, 10015–10043, 2014

Dependence of the CBT on soil moisture in the Chinese Loess Plateau and the adjacent areas

H. Wang et al.

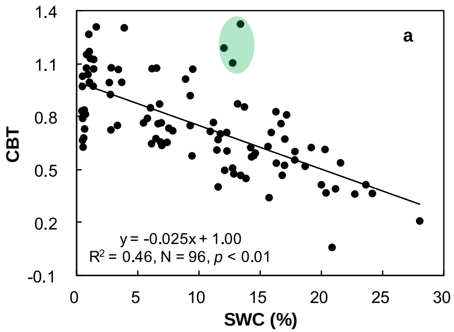


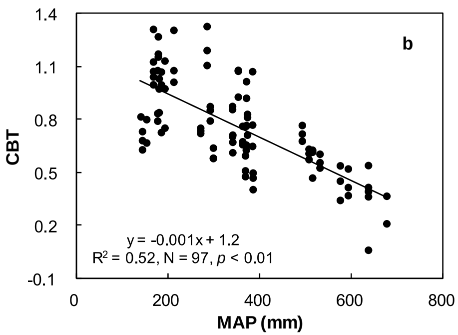


**Figure 4.** Plots showing the relationships of CBT with SWC **(a)** and MAP **(b)** for surface soils in this study. The light green shade in **(a)** indicates 3 Yongdeng soil samples collected immediately after a rainfall.





BGD
11, 10015–10043, 2014

Dependence of the CBT on soil moisture in the Chinese Loess Plateau and the adjacent areas

H. Wang et al.

Title Page
Abstract Introduction
Conclusions References
Tables Figures
◀ ▶
◀ ▶
Back Close
Full Screen / Esc
Printer-friendly Version
Interactive Discussion

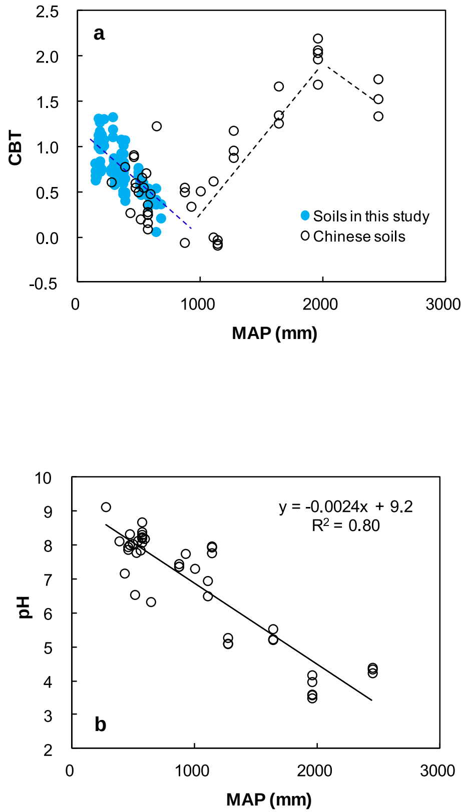


**Figure 5.** Correlations of local MAP with CBT **(a)** and soil pH **(b)** for Chinese surface soils (Xie et al., 2012). The MAP-CBT relationship for surface soils in this study was also indicated in **(a)** in the context of the results of Xie et al. (2012).

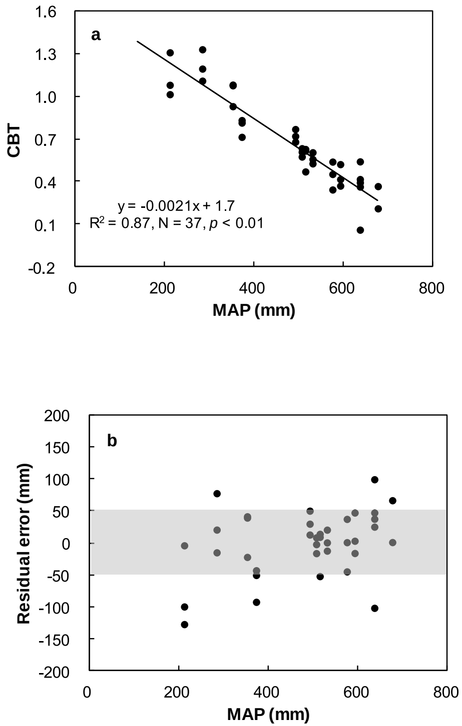


**Figure 6. (a)** Calibration plot of CBT values of surface soils in the CLP with local MAP. **(b)** MAP vs. residual MAP (meteorological MAP – estimated MAP using the surface soil calibration in the CLP). Gray shade marks the data within the RMSE (50 mm).

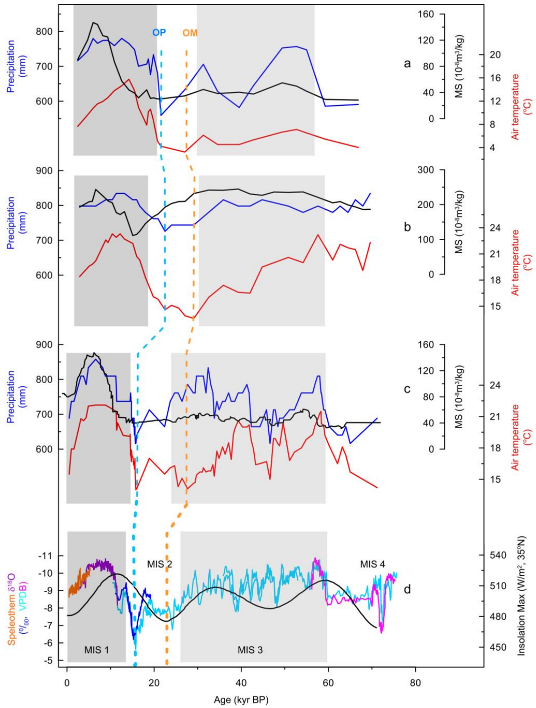


**Figure 7.** Comparison of variations in CBT-inferred MAP, bGDGT-derived temperature and magnetic susceptibility (MS) records of three LPSs sections **(a–c)** with speleothem-based EASM record (Wang et al., 2001, 2008) and local insolation (Huybers, 2006) **(d)**. The three LPSs sections are from Yuanbao (**a**, Jia et al., 2013), Lantian (**b**, Gao et al., 2012) and Mangshan (**c**, Peterse et al., 2014), respectively. The gray shade, light gray shade, blue dashed line, and orange dashed line indicate MIS 1, MIS 3, onset of precipitation enhancement (OP), and onset of Deglicial warming (OM), respectively.





BGD
11, 10015–10043, 2014

Dependence of the CBT on soil moisture in the Chinese Loess Plateau and the adjacent areas

H. Wang et al.

Title Page
Abstract | Introduction
Conclusions | References
Tables | Figures
◂◂ | ▸▸
◂ | ▸
Back | Close
Full Screen / Esc
Printer-friendly Version
Interactive Discussion